

## INTEGRATED ENVIRONMENTAL ASSESSMENT OF COASTAL VILLAGES IN THOOTHUKUDI DISTRICT: A GEOSPATIAL APPROACH FOR SUSTAINABLE COASTAL MANAGEMENT

A. Ernest Amita Roy<sup>1,2†</sup>, John Prince Soundranayagam<sup>1</sup>, A. Antony Alosanai Promilton<sup>3</sup>, V. Stephen Pitchaimani<sup>3</sup> and C. Antony Zacharius Grace<sup>1</sup>

<sup>1</sup>PG and Research Department of Physics, V.O. Chidambaram College, Thoothukudi 628008, India

<sup>2</sup>(Reg. No: 20112232132013) Research Scholar, Affiliated to Manonmaniam Sundaranar University, Tirunelveli-12, Tamil Nadu, India

<sup>3</sup>PG and Research Department of Geology, V.O. Chidambaram College, Thoothukudi 628008, India, Affiliated to Manonmaniam Sundaranar University, Tirunelveli-12, Tamil Nadu, India

†Corresponding Author: A. Ernest Amita Roy, Email: [amisartho@gmail.com](mailto:amisartho@gmail.com)

ORCID IDs: A. Ernest Amita Roy (0000-0003-1158-3160), John Prince Soundranayagam (0000-0001-7847-0895), A. Antony Alosanai Promilton (0000-0002-6762-0103), V. Stephen Pitchaimani (0009-0006-8560-1519) and C. Antony Zacharius Grace (0009-0005-7483-9161)

[https://doi.org/10.63001/tbs.2026.v21.i01.S.I\(1\).pp268-300](https://doi.org/10.63001/tbs.2026.v21.i01.S.I(1).pp268-300)

### KEYWORDS

*Integrated environmental assessment,  
Flood hazard,  
Groundwater potential,  
Urban heat island,  
Coastal vulnerability,  
Sustainable development.*

Received on: 23-12-2025

Accepted on: 08-02-2026

Published on:  
18-02-2026

### ABSTRACT

Coastal environments face unprecedented environmental pressures from urbanization, climate change and anthropogenic activities necessitating comprehensive integrated assessments for sustainable management. The study presents a comprehensive integrated environmental assessment of Thoothukudi District, Southern India utilizing hybrid TOPSIS-AHP multi-criteria decision analysis integrated with Google Earth Engine cloud computing to evaluate flood hazard, groundwater potential, land surface temperature and urban heat island dynamics. Technical assessments integrated twelve hydrological, topographic, geological and environmental parameters across coastal plain. Flood hazard assessment identified 64.50% (650.91 km<sup>2</sup>) moderate hazard coverage, 32.37% (326.62 km<sup>2</sup>) low hazard zones and 3.13% (31.61 km<sup>2</sup>) high hazard clusters concentrated near coastal villages. Groundwater potential mapping revealed 41.4% (405.37 km<sup>2</sup>) very high potential zones and 39.45% (386.24 km<sup>2</sup>) good potential areas supporting water-use efficiency and ecosystem protection. Land surface temperature analysis for 2025 documented pronounced seasonal variability with monsoon LST of 51.8°C, summer 39.4°C and winter 30.8°C, with spatial extremes ranging 9-78°C. Urban heat island intensity averaged 3.26°C in summer, 3.47°C during monsoon and 2.68°C in winter, with maximum values exceeding 24.93°C in urban cores. LULC classification revealed cropland dominance (487.0 km<sup>2</sup>, 48.3%), built-up areas (164.92 km<sup>2</sup>, 16.35%) and scrubland (197.82 km<sup>2</sup>, 19.61%). Composite vulnerability assessment identified low vulnerability zones occupying 88.14% (889.46 km<sup>2</sup>), moderate vulnerability 11.17% (112.71 km<sup>2</sup>) and high vulnerability 0.69% (6.97 km<sup>2</sup>) concentrated in coastal villages. The integrated framework provides spatially explicit evidence supporting SDGs 6, 11, 13, 14 and 15 enabling evidence-based coastal zone management, climate adaptation planning and sustainable development pathways.

## INTRODUCTION

Coastal zones represent critical interfaces between terrestrial and marine ecosystems, supporting approximately 40% of the global population while occupying less than 10% of terrestrial surface area and delivering essential ecosystem services including climate regulation, food security, biodiversity conservation and natural hazard buffering (Nyberg et al. 2025). The Indian subcontinent's extensive 7517 km coastline supports over 250 million inhabitants and exemplifies the global challenge of balancing economic development with environmental sustainability in coastal regions experiencing accelerated urbanization, agricultural intensification and climate-induced pressures (Ghosh & Mistri 2023). Coastal communities worldwide face escalating environmental risks from the convergence of climatic variability, sea-level rise, extreme weather events and intensifying anthropogenic pressures,

making them among the most vulnerable landscapes to hydro-meteorological disasters and environmental degradation (Bibi & Kara 2023; Gomez Rave, Scolobig & del Jesus 2025). Tamil Nadu's southeastern coastal districts, particularly Thoothukudi, exemplify these challenges where rapid urban-industrial expansion, intensive agriculture, aquaculture development and port operations create complex environmental pressures on fragile coastal ecosystems. Understanding the integrated environmental dynamics of these vulnerable coastal systems requires comprehensive assessments that simultaneously evaluate hydrological hazards, groundwater resources, thermal stress and land use transformations to support evidence-based sustainable development planning.

Traditional coastal environmental assessments have predominantly employed single-parameter or sector-specific

approaches that inadequately capture the complex interactions and feedback mechanisms between physical processes, hydrological systems, thermal dynamics and landscape transformations (Chowdhury et al. 2023). Flood risk assessment methodologies often overlook groundwater vulnerability, while land use change analyses rarely integrate thermal implications or hydrological consequences, creating fragmented knowledge that limits holistic management strategies (Odiji et al. 2024). The integration of Geographic Information Systems (GIS), remote sensing technologies and Multi-Criteria Decision Analysis (MCDA) techniques has revolutionized environmental assessment by enabling comprehensive spatial analysis of diverse datasets with varying scales and formats, yet most studies continue to address individual environmental components rather than integrated system-level dynamics (Agr Sci-Tarim Bili & Aslan 2024; Huang et al. 2024). The advent of cloud-based geospatial computing

platforms, particularly Google Earth Engine has revolutionized large-scale environmental monitoring by providing unprecedented access to petabyte-scale satellite imagery archives and advanced analytical capabilities that enable integrated multi-temporal assessments across extensive coastal landscapes (Gorelick et al. 2017; Pérez-Cutillas et al. 2023). Advanced machine learning algorithms including Random Forest and Gradient Tree Boosting combined with hybrid MCDA approaches such as TOPSIS-AHP integration offer robust methodological frameworks for handling complex multi-parameter environmental assessments while maintaining transparency and interpretability essential for policy applications (Chaube et al. 2024).

The sustainable development paradigm has fundamentally transformed environmental management approaches, shifting focus from sector-specific interventions to integrated system-level strategies aligned with global Sustainable

Development Goals (SDGs) (UNDP 2025). Integrated coastal environmental assessment directly contributes to multiple SDG targets, particularly SDG 6 (Clean Water and Sanitation), SDG 11 (Sustainable Cities and Communities), SDG 13 (Climate Action), SDG 14 (Life Below Water) and SDG 15 (Life on Land), necessitating holistic assessment frameworks that consider water security, disaster resilience, climate adaptation and ecosystem conservation as interconnected objectives (Mansour et al. 2022; Nandi & Swain 2024). Recent advances in geospatial artificial intelligence and ensemble modelling techniques have enhanced the precision of environmental vulnerability mapping, enabling real-time monitoring and predictive assessment capabilities that support adaptive management strategies, yet the translation of these technological advances into actionable insights for local-scale coastal management remains challenging (Singha et al. 2024). The explicit integration of SDG indicators into

integrated environmental assessment frameworks represents an emerging research frontier essential for aligning environmental management with broader sustainability objectives and enabling evidence-based policy formulation (Qazi et al. 2025).

Thoothukudi coastal villages present a compelling research context due to their unique combination of natural vulnerability factors and anthropogenic stressors that collectively amplify environmental risk exposure (Aswin, Pitchaimani & Promilton 2025). The region experiences bi-modal monsoon patterns with tropical cyclone impacts, progressive coastal erosion and saltwater intrusion challenges, while simultaneously supporting intensive fishing activities, major port operations, salt production, thermal power generation, chemical industries and rapidly expanding urban settlements (Krishnan & Ramasamy 2024; TNSDMA 2024). The semi-arid to sub-humid tropical climate creates conditions

conducive to thermal stress, while the low-lying coastal plains with gentle eastward slopes along the coastline create complex hydrological dynamics that increase flood susceptibility during extreme rainfall events (Richard Abishek & Antony Ravindran 2023). Previous environmental assessments in the region have primarily relied on single-parameter approaches or simplified analyses that inadequately capture the complex interactions between flood dynamics, groundwater availability, thermal stress patterns and land use transformations, while the absence of validated, integrated methodologies applicable across similar data-scarce coastal regions of South India and Southeast Asia represents a critical knowledge gap hindering effective environmental management and climate adaptation strategies.

The study creates a detailed plan to assess the environmental dynamics of Thoothukudi coastal villages. The objectives are: (i) to map flood risk areas

using a method that combines technical, environmental and social factors to help reduce disaster risks; (ii) to find areas where groundwater can be recharged by analysing various factors like water flow and land features for better water management; (iii) to measure changes in land temperature and urban heat during different seasons using machine learning to help with climate adaptation; (iv) to study land use land cover to support sustainable land management and (v) to combine all findings into a framework that assesses environmental pressures, identifies key areas for action and provides guidance for sustainable coastal development in line with Sustainable Development Goals.

## **MATERIALS AND METHODS**

### **Study Area Description**

The study area encompasses approximately 1009.14 km<sup>2</sup> across eight taluks in Thoothukudi District, Tamil Nadu, India (8.31-9.13°N; 77.83-78.37°E), representing a critical hydrogeological zone where continental drainage meets the Bay

of Bengal (Figure 1). The coastal plain slopes gently eastward from 50 m above mean sea level to sea level along a 30 km coastline. Physiographically, alluvial deposits, sandy coastal formations and lateritic uplands create heterogeneous aquifer systems with varying permeability. Impermeable clay layers restrict water percolation, promoting surface flooding during monsoons. The semi-arid to sub-humid tropical climate features monsoonal patterns with 800-1200 mm annual precipitation, concentrated during the northeast monsoon (October-December), which contributes 60% of annual rainfall with intense events exceeding 100 mm/day triggering coastal flooding. Temperature ranges from 24-38°C with consistently high humidity (70-85%).

Geomorphological diversity includes flood plains (6.36%), coastal plains (44.48%), deltaic plains (1.47%), aeolian sand dunes (3.13%) and pediment-pediain complexes (28.92%), each with distinct hydrological and hazard characteristics. Five major soil types dominate such as Entisols (52.39%) with high runoff and flood hazard, Vertisols (36.82%) with poor drainage intensifying ponding and Alfisols, Inceptisols and forest soils comprising remaining areas. The region supports 1.2 million people with population densities ranging from 100-30000 persons/km<sup>2</sup>. Rapid urbanization over two decades has increased impervious surfaces, reduced infiltration, accelerated runoff and disrupted natural flood attenuation mechanisms, creating complex environmental challenges.

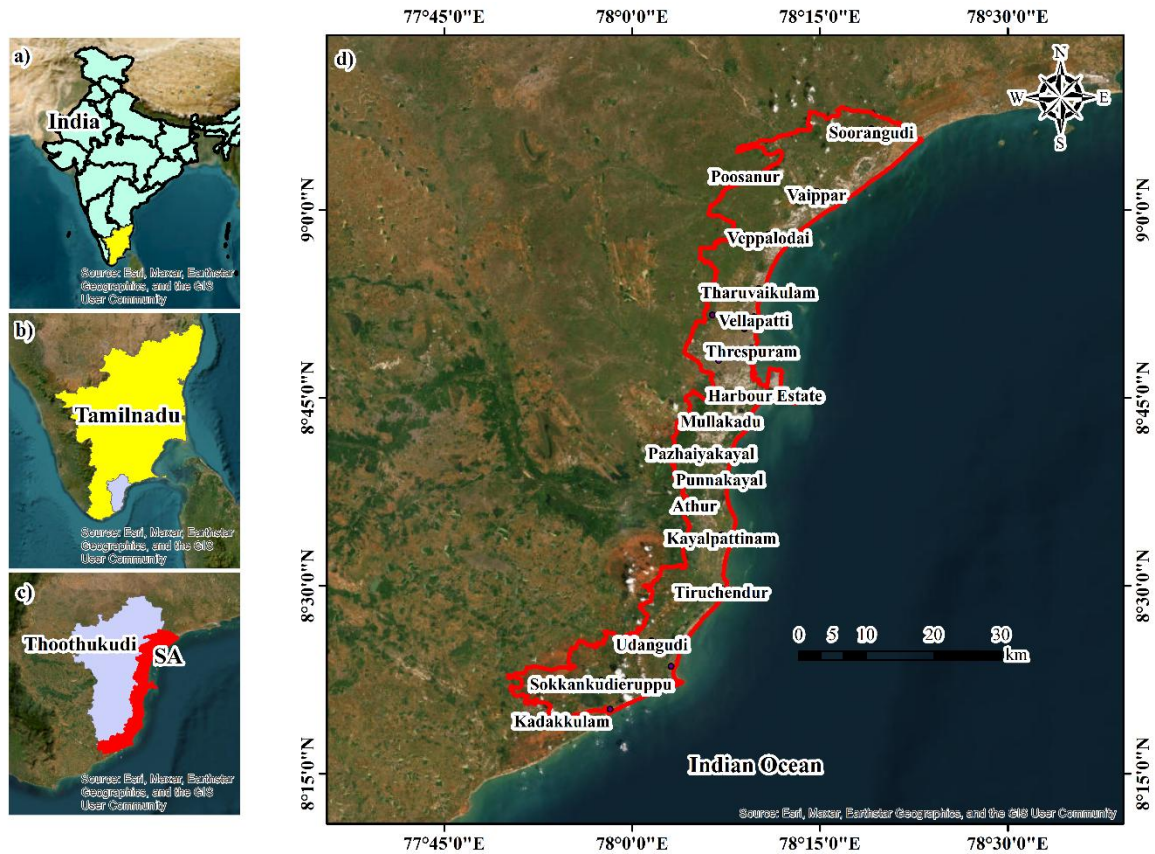


Figure 1. Location map of the study area

### Flood Hazard Assessment

A hybrid TOPSIS-AHP multi-criteria decision analysis evaluated ten parameters spanning technical, environmental and socioeconomic dimensions. Technical parameters included Topographic Wetness Index (TWI) from SRTM 30m DEM, elevation and proximity to waterbodies (GSI layers) representing physical flood susceptibility. Environmental parameters comprised rainfall data (IMD AARF 2019-2024, 0.25°

resolution), geomorphology (GSI 1:50,000), land use/land cover (Sentinel-2, 10m) and soil type (NBSS-LUP 1:250,000) describing conditions influencing flood generation and infiltration. Socioeconomic parameters included built-up density (Open Buildings 2.5D), proximity to roads (OpenStreetMap) and literacy exposure (Census 2011) capturing human vulnerability and adaptive capacity. The Analytical Hierarchy Process (AHP)

determined parameter weights through expert consultation using Saaty's pairwise comparison scale (CR=0.094). Normalized weights were: Rainfall (0.17), TWI (0.12), Geomorphology (0.12), LULC (0.11), Elevation (0.11), Proximity to Waterbodies (0.11), Soil Type (0.10), Built-up Density (0.06), Road Proximity (0.05) and Literacy Exposure (0.05). TOPSIS methodology ranked alternatives based on geometric distance from ideal solutions, generating relative closeness coefficients (0.19-0.80) representing flood hazard levels (Mitra, Das & Kamruzzaman 2023).

### **Groundwater Potential Recharge Assessment**

A hybrid TOPSIS-AHP approach integrated twelve factors across hydrological, topographic, geological and environmental categories. Hydrological factors included precipitation (IMD, 0.25° resolution), drainage density (SRTM-DEM 30m), proximity to waterbodies (Bhukosh-GSI 1:50,000) and groundwater table depth (WRIS-India) quantifying recharge input

and surface-groundwater interactions. Topographic factors elevation, slope and Topographic Wetness Index (SRTM-DEM) governed infiltration opportunity time. Geological factors comprised lithology (Bhukosh-GSI 1:50,000), soil texture (NBSS-LUP 1:250,000) and geomorphology characterizing subsurface permeability and porosity. Environmental factors included land use/land cover (ESRI World Land Cover Atlas 10m) and Normalized Difference Vegetation Index (Landsat-8 OLI 30m) capturing infiltration-runoff partitioning and evapotranspiration dynamics. AHP pairwise comparison established normalized factor weights: Precipitation (0.12), Water Table Depth (0.10), LULC (0.10), Lithology (0.09), TWI (0.09), Slope (0.08), Geomorphology (0.08), Drainage Density (0.08), Proximity to Water Bodies (0.08), Soil Texture (0.06), NDVI (0.06) and Elevation (0.06), with CR=0.058 confirming consistency (Saaty 1987). TOPSIS derived relative closeness coefficients (Ci: 0-1) classifying

groundwater potential as Excellent ( $C_i > 0.8$ ), Very High (0.6-0.8), Good (0.4-0.6), Moderate (0.2-0.4) and Low ( $C_i < 0.2$ ) (Opricovic & Tzeng 2004; Purmohammadi et al. 2024).

### **Land Surface Temperature and Urban Heat Island Assessment**

Landsat 8/9 data for 2025 were processed in Google Earth Engine to assess seasonal land surface temperature (LST) and urban heat island (UHI) dynamics across three periods: summer (March-May), monsoon (June-September) and winter (December-February). Seasonal composite images were generated using median pixel values with cloud cover <10% threshold to minimize atmospheric interference (Gorelick et al. 2017). LST retrieval involved radiometric conversion of Band 10 thermal data to at-sensor spectral radiance, brightness temperature calculation through Planck's inverse function ( $K_1 = 774.8853 \text{ W} \cdot \text{m}^{-2} \cdot \text{sr}^{-1} \cdot \mu\text{m}^{-1}$ ;  $K_2 = 1321.0789 \text{ K}$ ), emissivity correction accounting for surface heterogeneity

through proportion of vegetation derived from NDVI ( $\text{NDVI}_{\min} = 0.2$ ,  $\text{NDVI}_{\max} = 0.7$ ) and final LST calculation with wavelength-dependent Planck function ( $\lambda = 11.0 \mu\text{m}$ ,  $\rho = 1.438 \times 10^{-2} \text{ m} \cdot \text{K}$ ) (Chandu, Bindu & Vishnu Sharan K. J 2025). Urban heat island intensity was calculated as  $\text{LST}_{\text{urban}} - \text{LST}_{\text{rural}}$  (25th percentile LST values).

### **Land Use/Land Cover Dynamics**

LULC classification for 2025 employed Landsat 8/9 OLI satellite imagery with minimal cloud cover (<10%) acquired during post-monsoon season (January-February) for optimal vegetation phenology. Seven LULC classes were defined: Water Bodies (rivers, ponds, reservoirs, aquaculture), Forest (tree cover >10% canopy density), Flooded Vegetation (seasonally waterlogged areas with emergent vegetation), Cropland (irrigated and rainfed agricultural lands), Built-up Areas (residential, commercial, industrial and transportation infrastructure), Barren Areas (exposed soil, sandy areas, rocky

outcrops, fallow lands) and Scrub Land (shrubland, degraded forest, sparse xerophytic vegetation) (Shahfahad et al. 2024). Random Forest classifier was selected for its superior performance in complex coastal environments, constructing multiple decision trees with optimization parameters: 500 trees, minimum leaf population=5 and variables per split equal to square root of total input variables (Faheem et al. 2024). Training samples (350 total: 50 per class) were collected through stratified random sampling combining high-resolution imagery interpretation, field surveys with handheld GPS and false colour composite analysis. Classification accuracy was evaluated using 350 independent validation points (50 per class) stratified randomly across the study area. Error matrices were constructed to calculate overall accuracy, user's accuracy, producer's accuracy and Kappa coefficient. The 2025 classification achieved 93.71% overall accuracy ( $\kappa=0.92$ )

demonstrating excellent classification performance.

### **Integrated Environmental Assessment Framework**

Spatial overlay analysis in ArcGIS 10.8 integrated georeferenced thematic layers from flood hazard mapping, groundwater potential recharge zone, thermal stress analysis and LULC classification to evaluate cumulative environmental pressures and identify priority intervention zones supporting sustainable coastal management. The layers were normalized to 30m resolution and WGS 1984 UTM Zone 44N projection. Composite Vulnerability Index (CVI) was calculated as (Antony et al. 2024):

$$\begin{aligned}
 CVI = & 0.30 \times Flood\ Hazard \\
 & + 0.25 \times GWPRZ \\
 & + 0.25 \times UHII \\
 & + 0.20 \times LULC
 \end{aligned}$$

where weights reflect relative importance of disaster risk (30%), water scarcity (25%), thermal stress (25%) and land degradation (20%) based on expert

consultation. Village-level aggregation employed zonal statistics (mean, maximum, standard deviation) within administrative boundaries enabling comparative assessment and priority ranking for targeted interventions.

Environmental findings were aligned with Sustainable Development Goals: flood risk mapping supports SDG 11.5 (disaster risk reduction) and SDG 13.1 (climate adaptation); groundwater potential assessment contributes to SDG 6.4 (water-use efficiency) and SDG 6.6 (water-related ecosystems); thermal stress analysis informs SDG 11.6 (environmental quality) and SDG 13.2 (climate measures); and LULC change detection supports SDG 14.2 (marine ecosystems) and SDG 15.3 (land degradation neutrality). The framework provides spatially explicit guidance for priority interventions including artificial recharge infrastructure in high flood-high groundwater potential zones, urban heat mitigation in vegetated sparse areas, green infrastructure planning in built-up

expansion zones, ecosystem conservation and climate-resilient development pathways (United Nations Department of Economic and Social 2024).

## RESULTS

### Flood Hazard

The integrated flood hazard assessment reveals extensive moderate-risk coverage with 64.50% (650.91 km<sup>2</sup>) of the study area exhibiting medium hazard levels, while low hazard zones comprise 32.37% (326.62 km<sup>2</sup>) concentrated inland at higher elevations (>10m) with robust drainage networks (Figure 2). High hazard occupy 3.13% (31.61 km<sup>2</sup>) sharply concentrated near Athur, Punnakayal and Soorangudi within 2 km of the coastline and major river corridors where compound flooding from tidal and precipitation interplay creates known hotspots (Norizan, Hassan & Yusoff 2021). Topographic Wetness Index analysis shows moderate hazard zones dominating 58.67% (592.04 km<sup>2</sup>) with high hazard regions covering 8.73% (88.09 km<sup>2</sup>) focused around low-

lying catchments where natural drainage pathways converge. Elevation reveals 77.87% (785.86 km<sup>2</sup>) in moderate to high flood hazard zones (3-20m) encompassing key settlements including Athur, Tiruchendur, Millerpuram and Kayalpattinam consistently experiencing compound flooding, while the lowest elevation (<3m, 135.79 km<sup>2</sup>, 13.46%) including Sakkankudieruppu and Pazhaiyakayal exhibits maximum vulnerability from tidal surges and cyclone-induced storm waves (Zope, Eldho & Jothiprakash 2015).

Spatial parameter analysis demonstrates distinct hazard heterogeneity across physiographic and hydrological dimensions. Proximity to waterbodies shows 36.67% (370.03 km<sup>2</sup>) within 750m of major water bodies forming very high hazard belts near Vaippar, Veppalodai, Harbour Estate, Athur, Punnakayal and

Tiruchendur repeatedly impacted by seasonal flooding. Rainfall distribution reveals highest hazard concentration (1065-1085 mm) near Athur, Punnakayal and Soorangudi where monsoon-driven pluvial flooding peaks, while moderate hazard areas (960-1025 mm) comprise 31.80% (320.87 km<sup>2</sup>). Geomorphological analysis identifies flood plains (6.36%) concentrated near Poosanur, Vaippar and Athur posing very high hazard, coastal plains (44.48%) enveloping numerous villages with elevated vulnerability and deltaic plains (1.47%) near Punnakayal prone to tidal backwatering. Land use analysis shows settlement zones (16.12%) and croplands (47.64%) representing high and moderate hazard respectively, with flooded vegetation consistently aligning with very high hazard due to persistent inundation regimes (Xue et al. 2024).

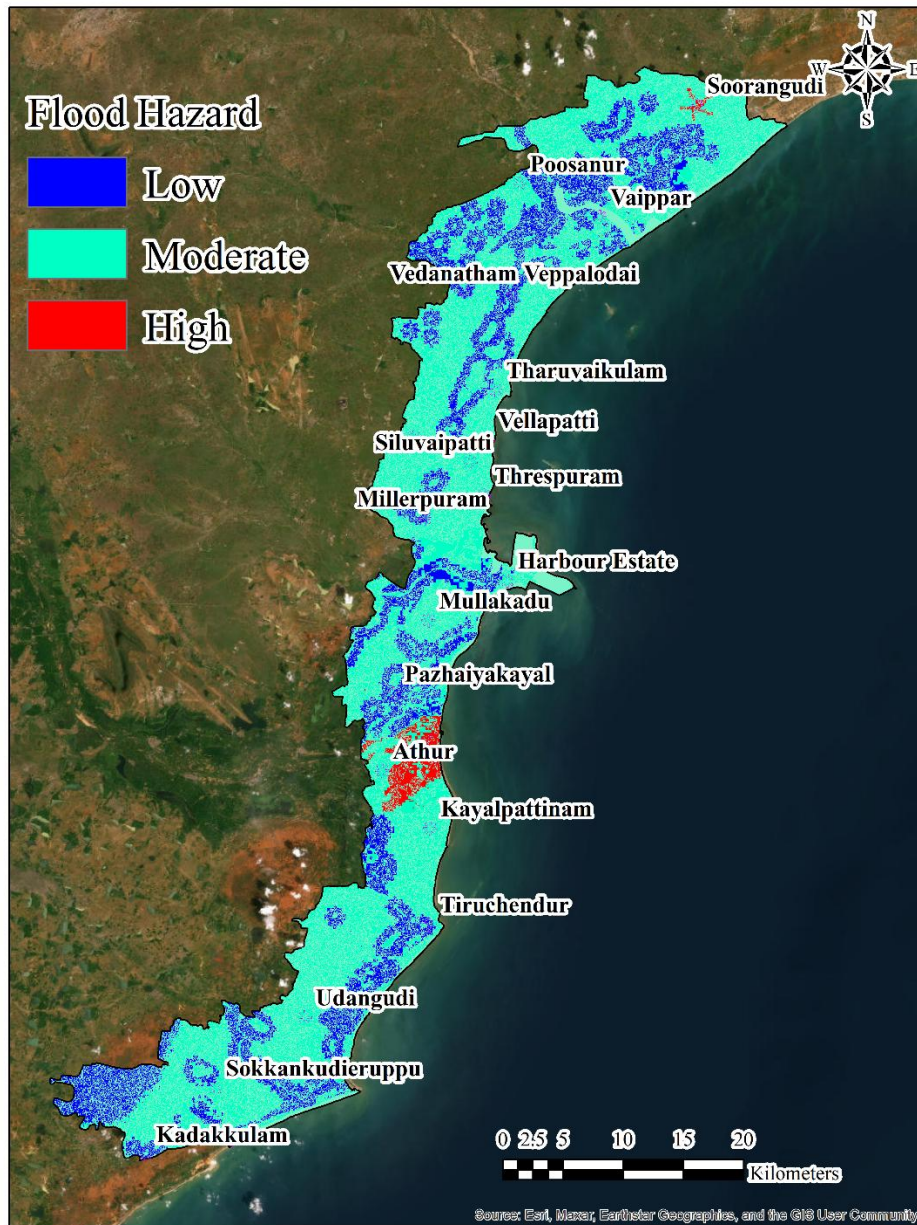


Figure 2. Flood Hazard Map of the Study Area

### Groundwater Potential Recharge Zone

The groundwater potential assessment reveals significant spatial heterogeneity with Very High Potential zones covering 41.4% (405.37 km<sup>2</sup>) predominantly in central coastal transition villages including Vaippar, Veppalodai,

Kayalpattinam, Athur and Punnakayal (Figure 3). Good Potential zones comprise 39.45% (386.24 km<sup>2</sup>) across agricultural areas and southern regions, Moderate Potential zones occupy 14.48% (141.80 km<sup>2</sup>), Low Potential areas cover 3.52%

(34.47 km<sup>2</sup>) and Excellent Potential zones constitute 1.15% (11.26 km<sup>2</sup>) in high-infiltration localities. Factor analysis demonstrates precipitation highest in central coastal villages (1175-1298 mm, 14%) supporting excellent recharge, while lowest rainfall zones (812-910 mm, 28%) indicate low potential requiring supplementary recharge (Zhu & Abdelkareem 2021). Drainage density shows low density zones (0-0.558 km/km<sup>2</sup>, 18%) exhibit excellent potential through enhanced infiltration, moderate density areas (0.933-1.261 km/km<sup>2</sup>, 29%) represent good potential and high density zones (1.675-2.454 km/km<sup>2</sup>, 4%) show low potential. Proximity to waterbodies reveals 36.59% within 681m exhibiting excellent potential through bank infiltration mechanisms, 30.3% in 681-1385m buffer showing very high potential, while areas beyond 3338m (3.66%) indicate low potential. Groundwater table depth analysis shows shallow zones (0-3m, 4.3%) offer excellent potential, optimal depths (3-6m,

41.56%) demonstrate very high potential and deep water table areas (>15m, 4.79%) indicate low potential with high extraction costs.

Topographic and lithological analysis reveals low elevation zones (-14 to 8m, 41.88%) exhibit excellent recharge potential, gentle slopes (0-2°, 80.34%) provide excellent infiltration opportunity, while steep slopes (>15°, 0.17%) demonstrate low potential. Topographic Wetness Index shows high values (18.26-25.67, 2.93%) indicate excellent potential in water accumulation zones, moderate TWI areas (13.23-15.47, 18.48%) represent good potential and low TWI zones (43.98%) show low potential requiring artificial recharge (Maqsoom et al. 2022). Lithological analysis demonstrates coarse sand and limestone formations (1.35%) exhibit excellent permeability, sand dunes (16.52%) and paleo beach ridges (4.96%) show very high potential, while black clay and silty clay zones (24.37%) indicate low potential. Soil texture reveals Entisols

(53.64%, 521.02 km<sup>2</sup>) exhibit excellent potential with sandy texture facilitating infiltration, Vertisols (35.09%) demonstrate moderate potential and Alfisols (3.85%) show very high potential. Geomorphological analysis shows aeolian sand dunes and sheets (4.34%) exhibit excellent potential, coastal plains (43.78%, 423.4 km<sup>2</sup>) demonstrate very high potential as primary recharge zones, pediment-

pediplain complexes (28.92%) represent good potential, while salt pans (9.54%) indicate low potential. Land use analysis reveals water bodies (6.31%) offer excellent direct infiltration potential, cropland (47.64%) represents good potential through irrigation returns, while built-up areas (16.12%) show low potential due to impervious surfaces (Nazaripour et al. 2024).

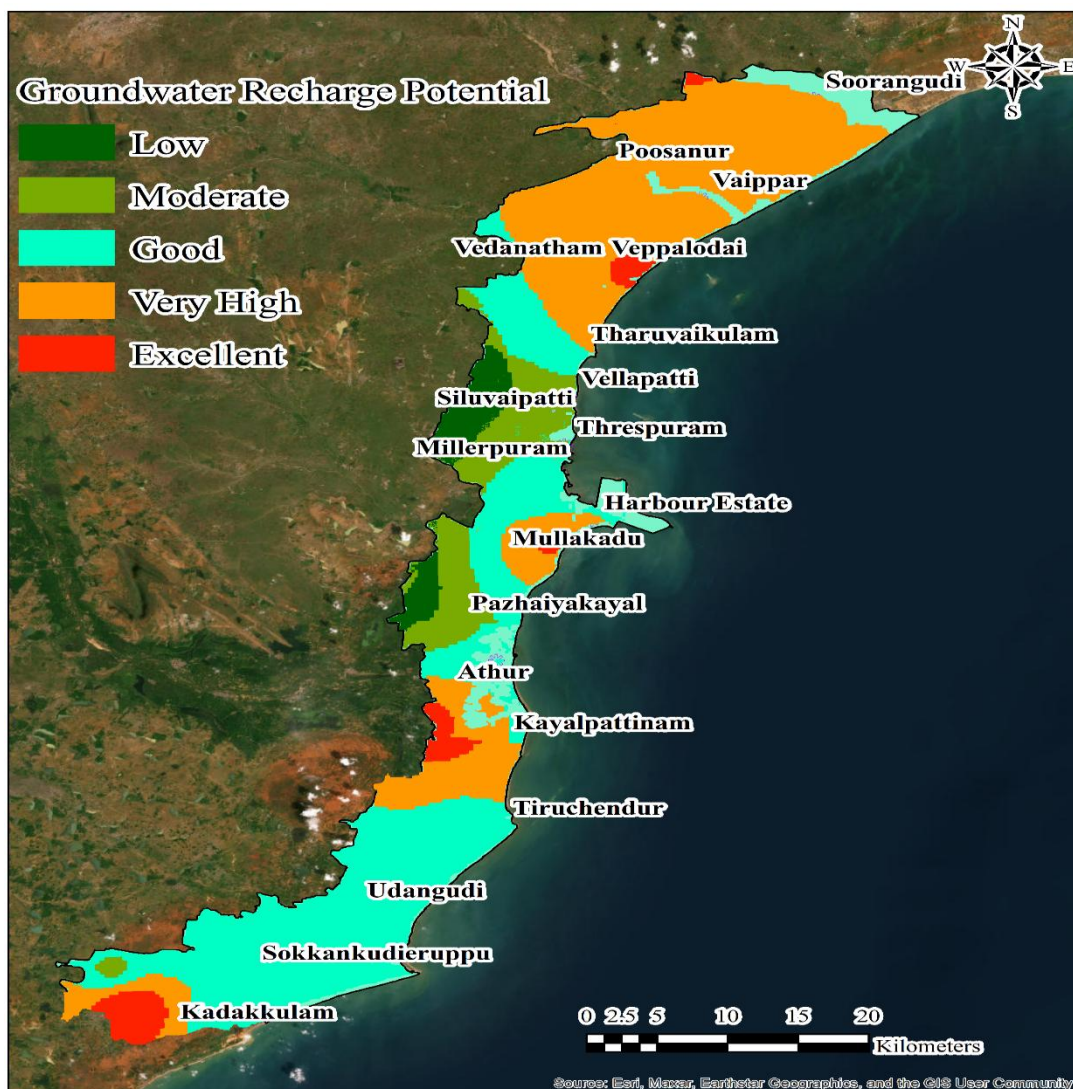


Figure 3. Groundwater Recharge Potential Map of the Study Area

### Land Surface Temperature and Urban Heat Island Dynamics

Seasonal land surface temperature analysis for 2025 reveals pronounced seasonal variability with mean LST values demonstrating clear stratification: monsoon LST reached 51.8°C, substantially higher than summer values of 39.4°C, while winter LST remained consistently lower at 30.8°C (Figure 4 a&b). The magnitude of seasonal temperature difference between monsoon and winter approximates 19.8°C reflecting substantial seasonal climate cycle influence driven by precipitation patterns, cloud cover variation and solar radiation intensity (Kumar et al. 2017). Spatial heterogeneity analysis reveals pixel-level extremes ranging from 9°C to over 78°C, with highest LST's consistently clustering in urban cores and industrial areas approaching or exceeding 70°C due to low-albedo, high-thermal-capacity surfaces and vegetation loss in northern villages

including Soorangudi, Poosanur, Vaippar and Vedanatham. The water bodies, mangrove belts and vegetated districts dampen local maxima often exhibiting minimum LST values below 30°C in southern coastal villages including Sokkankudieruppu, Kadakkulam, Periyathalai, Udangudi and canal-adjacent areas near Tiruchendur. The spatial thermal range exceeds 60°C, vastly outpacing mean seasonal changes. Urban heat island intensity reveals average UHI values of 3.26°C in summer, 3.47°C during monsoon and 2.68°C in winter. Maximum UHI values exhibit spatial concentration with summer maximum reaching 24.93°C in urban cores, indicating intensification of extreme urban thermal anomalies in localized high-growth areas (El Afandi & Ismael 2023).

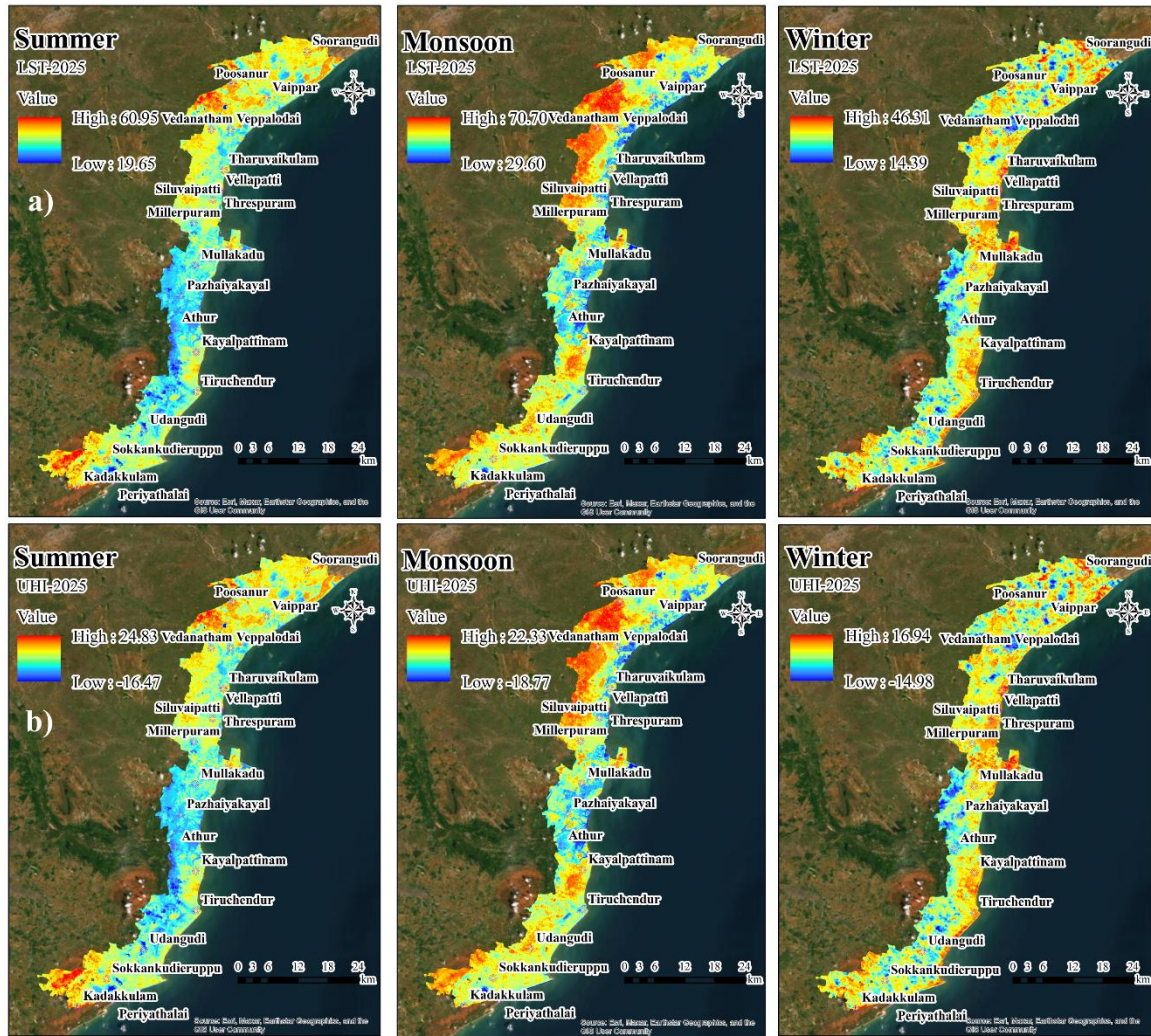


Figure 4. Seasonal a) LST and b) UHI Map of the Study Area

### Land Use/Land Cover Change Dynamics and Future Projections

The LULC classification reveals that Cropland dominated with 487.0 km<sup>2</sup> (48.3%) representing the most extensive class, concentrated in central and northern villages including Vedanatham and Soorangudi (Figure 5). Built-up areas covered 164.92 km<sup>2</sup> (16.35%) concentrated in urban cores of Tiruchendur,

Kayalpattinam, Millerpuram and peri-urban expansion zones reflecting population growth and infrastructure expansion. Scrubland occupied 197.82 km<sup>2</sup> (19.61%) with scattered distribution across inland villages. Water bodies comprised 82.38 km<sup>2</sup> (8.17%) including natural water bodies, irrigation tanks, reservoirs and

aquaculture ponds predominantly in coastal villages including Athur, Punnakayal, Kayalpattinam and Mullakadu. Barren areas covered 117.61 km<sup>2</sup> (11.65%) representing exposed soil, sandy areas and fallow lands primarily in northern and western portions. Forest cover occupied 33.08 km<sup>2</sup> (3.28%) comprising scattered forest patches and coastal vegetation, while flooded vegetation covered 6.93 km<sup>2</sup> (0.69%) in seasonally waterlogged areas. Classification accuracy achieved 93.71% overall accuracy ( $\kappa=0.92$ ) with class-specific user's and producer's accuracies exceeding 88% for major classes, confirming excellent classification reliability.

Spatial LULC distribution demonstrates distinct patterns reflecting environmental gradients and socioeconomic drivers across eight administrative taluks. Northern villages (Soorangudi, Poosanur, Vaippar, Vedanatham) exhibit higher built-up density and agricultural intensification with

dense cropland coverage. Central villages (Tharuvaikulam, Vellapatti, Siluvaipatti, Athur) display mixed land use including significant cropland expansion, moderate built-up areas and water body proliferation supporting aquaculture activities. Southern coastal settlements (Kayalpattinam, Tiruchendur, Udangudi, Periyathalai, Sokkankudieruppu) show higher proportions of water bodies, natural vegetation and lower built-up coverage due to coastal constraints. The spatial heterogeneity reflects contemporary landscape dynamics driven by agricultural intensification, coastal aquaculture development and differential urbanization pressures across administrative boundaries. This creates complex environmental mosaics with varying hydrological, thermal and ecological characteristics influencing flood susceptibility, groundwater dynamics and thermal stress patterns across the coastal plain (Xu et al. 2021).

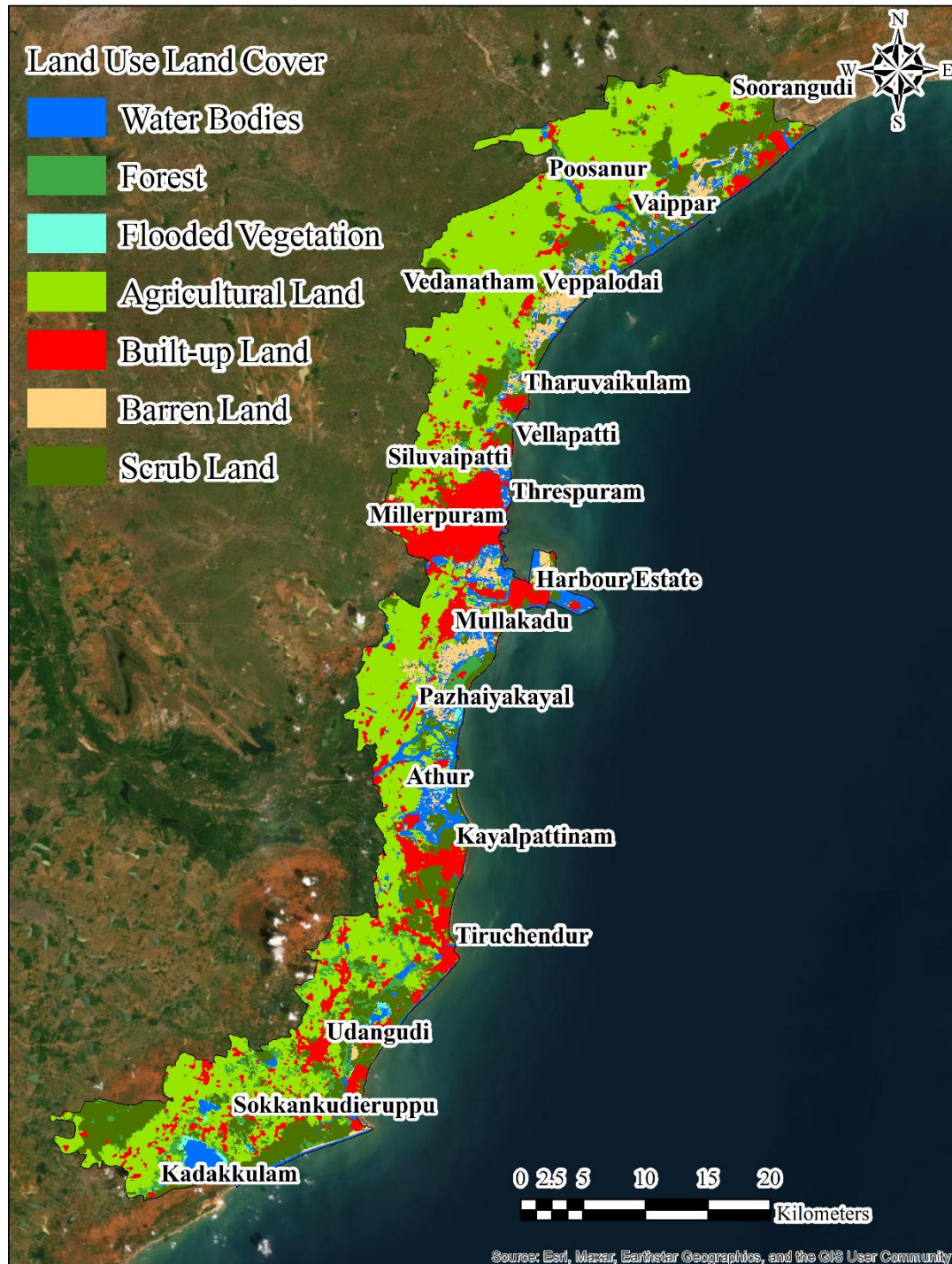


Figure 5. Land Use Land Cover Map of the Study Area

### Integrated Environmental Vulnerability Assessment

Spatial overlay analysis of the four environmental assessment components reveals distinct vulnerability patterns across

the study area (Table 1). Composite Vulnerability Index (CVI) analysis identifies three vulnerability categories:

Low Vulnerability zones dominate with 88.14% (889.46 km<sup>2</sup>) distributed predominantly across southern and inland villages including Sakkankudieruppu, Kadakkulam, Periyathalai, Vedanatham, Veppalodai, Poosanur and Soorangudi, where favorable combinations of manageable flood hazards, high groundwater potential, moderate thermal stress and substantial natural vegetation cover provide environmental resilience. Moderate Vulnerability zones comprise 11.17% (112.71 km<sup>2</sup>) concentrated in central coastal villages including Tiruchendur, Mullakadu, Siluvaipatti, Udangudi, Tharuvaikulam and Vellapatti, where moderate flood hazards, good

groundwater availability, moderate thermal stress and mixed land use patterns create transitional conditions amenable to proactive management. High Vulnerability zones occupy only 0.69% (6.97 km<sup>2</sup>) sharply concentrated in densely populated coastal villages including Athur, Punnakayal and Kayalpattinam where convergence of high flood risk, low groundwater potential, intense urban heat islands and extensive built-up imperviousness create compound environmental pressures requiring urgent integrated intervention. Village-level analysis reveals distinct environmental profiles enabling targeted management.

Table 1: Composite Vulnerability Index (CVI) Classification

Vulnerability Class	Area (km <sup>2</sup> )	Percentage (%)	Threshold Range
Low Vulnerability	889.46	88.14	CVI ≤ 0.40
Moderate Vulnerability	112.71	11.17	0.40 < CVI ≤ 0.60
High Vulnerability	6.97	0.69	CVI > 0.60

High vulnerability villages including Athur (densest clustering) and Punnakayal face compound pressures from very high flood risk, moderate groundwater potential, intense urban heat islands (UHII  $>4.0^{\circ}\text{C}$ ) and substantial built-up expansion, requiring comprehensive integrated management including flood-resistant infrastructure, artificial recharge facilities, urban greening programs and controlled development zoning (Figure 6). Moderate vulnerability villages including Tiruchendur, Mullakadu and Tharuvaikulam demonstrate balanced environmental conditions but face emerging pressures from agricultural intensification and urban growth, providing opportunities for proactive sustainable development integrating green corridors, aquifer protection zones and climate-

resilient infrastructure. Low vulnerability villages benefit from favorable environmental conditions including low flood exposure, high groundwater potential, moderate thermal stress and extensive natural vegetation, yet face future pressures from projected development requiring precautionary conservation strategies. Critical thematic integration reveals flood-groundwater nexus where high flood hazard zones coincide with very high groundwater potential, enabling managed aquifer recharge through flood water harvesting. Urban heat-vegetation dynamics demonstrate strong inverse relationship confirming vegetation cooling effectiveness, supporting ecosystem-based adaptation strategies.

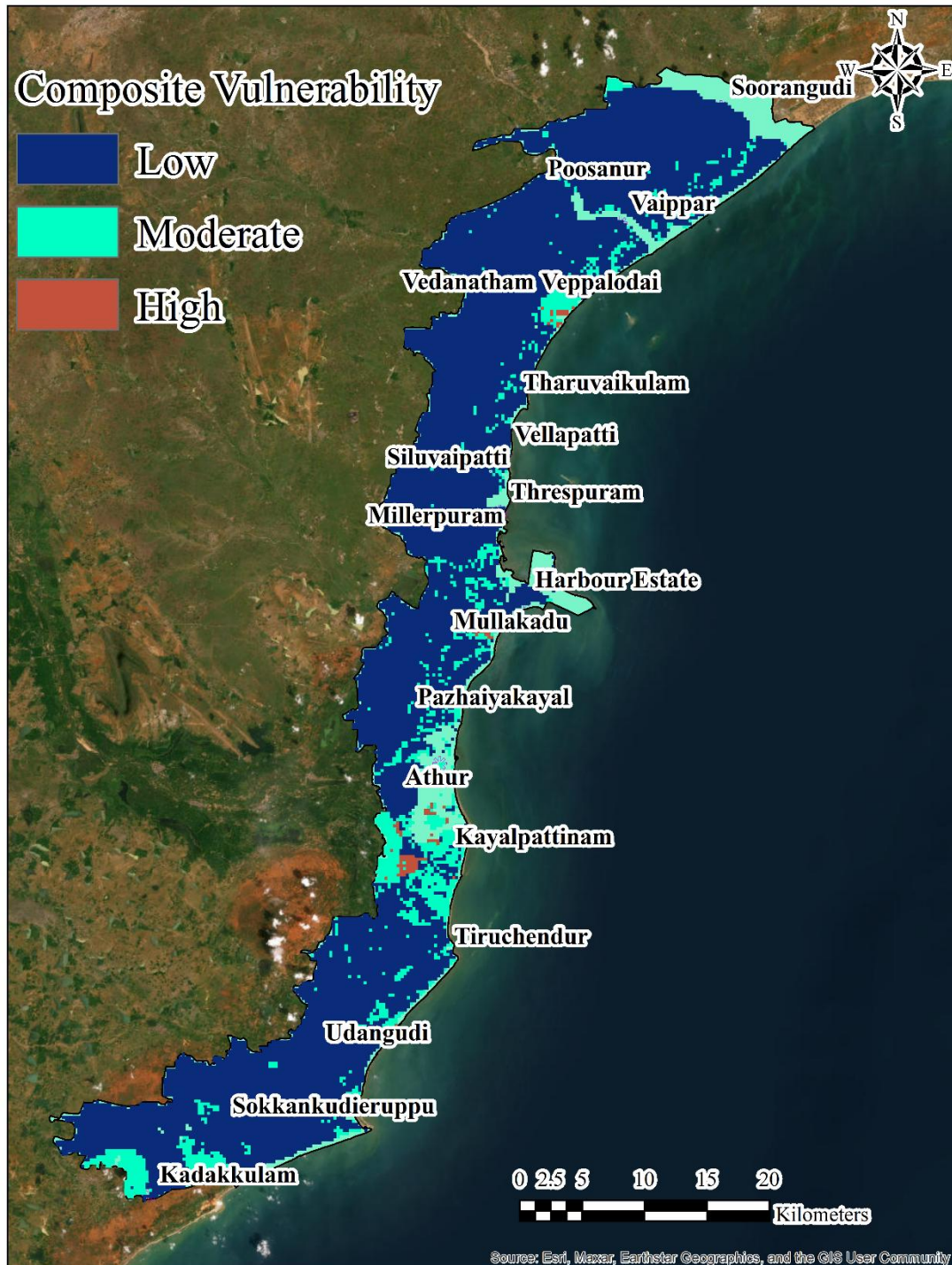


Figure 6. Composite Vulnerability Index Map of the Study Area

## DISCUSSION

### Comparative Perspectives

The hybrid TOPSIS-AHP methodology integrated with Google Earth

Engine cloud computing represents a significant methodological advancement

over conventional single-parameter coastal assessments reported in similar tropical coastal environments. While previous studies in Tamil Nadu's coastal districts have predominantly employed individual hazard assessments or dual-parameter approaches with the present framework's simultaneous integration of flood hazard, groundwater dynamics, thermal stress and land use transformations reveals critical interdependencies typically overlooked in sectoral analyses. The negative correlation ( $r = -0.58$ ) between flood hazard and groundwater potential zones particularly illuminates opportunities for nature-based solutions where flood-prone areas coincide with high infiltration capacity is a synergy rarely quantified in South Asian coastal vulnerability literature. The several methodological limitations warrant acknowledgment. The static nature of current LULC classification does not capture rapid seasonal transformations characteristic of monsoon-influenced tropical coasts, potentially underestimating

temporal vulnerability fluctuations. The absence of subsurface geological heterogeneity data and time-series groundwater level measurements limits the precision of recharge zone delineation in fractured crystalline basement aquifers that dominate the study area. Future iterations should incorporate multi-temporal Synthetic Aperture Radar interferometry for subsidence monitoring, ensemble climate projections for forward-looking vulnerability scenarios and participatory GIS approaches to integrate indigenous coastal knowledge systems into formal assessment frameworks.

### **Sustainable Development Goals Alignment and Policy Implications**

The integrated environmental assessment provides spatially explicit evidence supporting multiple Sustainable Development Goal targets with direct policy implications for coastal management. SDG 6 (Clean Water and Sanitation) implementation benefits from groundwater potential mapping identifying

405.37 km<sup>2</sup> (41.4%) very high potential zones and 386.24 km<sup>2</sup> (39.45%) good potential zones for managed aquifer recharge infrastructure targeting SDG 6.4 (water-use efficiency) and SDG 6.6 (water-related ecosystems protection). Strategic recharge sites overlap with flood-prone areas enabling dual-purpose infrastructure for flood mitigation and aquifer replenishment (Aloui et al. 2024). SDG 11 (Sustainable Cities and Communities) advancement occurs through flood risk mapping identifying 104.17 km<sup>2</sup> (10.32%) high-risk zones requiring urgent intervention for SDG 11.5 (disaster risk reduction), thermal stress analysis quantifying urban heat impacts affecting 15-20% of areas supporting SDG 11.6 (environmental quality improvement) and LULC patterns guiding sustainable expansion pathways for SDG 11.3 (inclusive urbanization). The dominance of low vulnerability zones (88.14%, 889.46 km<sup>2</sup>) across southern and inland villages provides favorable conditions for

sustainable development with environmental resilience, while the spatial concentration of high vulnerability (0.69%, 6.97 km<sup>2</sup>) in northern coastal villages including Athur and Punnakayal enables targeted intervention prioritization (Allan, Rajabifard & Foliente 2024). SDG 13 (Climate Action) operationalization integrates thermal analysis documenting urban heat island intensification and land use transformations supporting SDG 13.1 (strengthen climate resilience and adaptive capacity), while integrated vulnerability assessment identifies priority adaptation zones requiring nature-based solutions for SDG 13.2 (integrate climate change measures).

SDG 14 (Life Below Water) contributions emerge through coastal land use monitoring documenting water body expansion (82.38 km<sup>2</sup>, 8.17% in 2025) including aquaculture development and ecosystem transformation pressures supporting SDG 14.2 (sustainable management of marine and coastal

ecosystems). SDG 15 (Life on Land) advancement through LULC characterization quantifying terrestrial ecosystem distributions including forest cover (33.08 km<sup>2</sup>, 3.28%), scrubland (197.82 km<sup>2</sup>, 19.61%) and vegetation patterns supporting SDG 15.3 (combat land degradation and restore degraded lands) (Arora & Mishra 2024). Cross-cutting contributions address SDG 1.5 (build resilience of vulnerable populations) through vulnerability integration emphasizing spatial distribution of exposed communities, SDG 3.9 (reduce deaths from hazardous conditions) via thermal and flood risk mapping identifying health-vulnerable zones and SDG 9.1 (develop quality, reliable, sustainable infrastructure) through spatially explicit planning guidance (Fourie 2022; Halkos & Argyropoulou 2022). Priority policy recommendations include village-level Integrated Coastal Zone Management plans with flood risk zoning and ecosystem conservation, nature-based solutions targeting high vulnerability zones,

managed aquifer recharge programs in flood-groundwater nexus zones, early warning systems protecting vulnerable populations and climate-adaptive land use regulations restricting development in high cumulative vulnerability areas while promoting green space and ecosystem restoration.

## CONCLUSION

The integrated environmental assessment of Coastal villages of Thoothukudi District reveals a predominantly resilient coastal landscape with spatially concentrated vulnerability in densely populated areas. The research demonstrates that 88.14% of the study area exhibits low vulnerability characterized by favorable combinations of manageable flood hazards, high groundwater potential, moderate thermal stress and substantial natural vegetation cover. This dominance of low vulnerability zones provides a foundation for sustainable development with environmental resilience across southern and inland villages including

Sokkankudieruppu, Kadakkulam, Vedanatham and Poosanur. However, critical hotspots exist where compound environmental pressures converge. High vulnerability zones (0.69%, 6.97 km<sup>2</sup>) concentrated in northern coastal villages including Athur, Punnakayal and Kayalpattinam face convergent flood risk, groundwater stress, intense urban heat islands (UHII >4.0°C) and extensive built-up imperviousness, requiring urgent integrated interventions. The spatial analysis reveals critical environmental synergies enabling multi-purpose infrastructure development. The flood-groundwater nexus ( $r = -0.58$ ) demonstrates that high flood hazard zones often coincide with very high groundwater potential areas, creating opportunities for managed aquifer recharge through flood water harvesting infrastructure including check dams, percolation tanks and recharge wells simultaneously addressing flood mitigation and water security.

The strong inverse urban heat-vegetation relationship confirms that nature-based solutions provide co-benefits for thermal stress reduction, flood attenuation and groundwater recharge improvement. The 2025 LULC assessment documenting 48.3% cropland, 16.35% built-up areas and 19.61% scrubland provides baseline characterization for sustainable land management integration. Priority policy implementation should focus on: (i) village-level Integrated Coastal Zone Management plans incorporating flood risk zoning, groundwater protection zones and ecosystem conservation; (ii) nature-based solutions including urban forest development in high vulnerability zones and green-blue infrastructure corridors; (iii) managed aquifer recharge programs strategically siting infrastructure in overlapping flood-groundwater potential zones; (iv) early warning systems protecting vulnerable populations in high-risk flood areas; and (v) climate-adaptive

land use regulations restricting development in high vulnerability zones while promoting green space integration and ecosystem restoration. The research directly supports Sustainable Development Goals 6 (clean water and sanitation), 11 (sustainable cities), 13 (climate action), 14 (life below water) and 15 (life on land), providing spatially explicit evidence for transformative coastal zone management policies balancing environmental protection with sustainable development objectives.

#### **ACKNOWLEDGEMENT**

The authors acknowledge the Indian Meteorological Department (IMD), Geological Survey of India (GSI), National Bureau of Soil Survey and Land Use Planning (NBSS-LUP), Water Resources Information System of India (WRIS) and United States Geological Survey (USGS) for providing datasets used in this study. The Google Earth Engine platform is acknowledged for cloud computing support. The First author expresses his

sincere thanks to Shri. A.P.C.V. Chockalingam, Secretary and our Principal, V. O. Chidambaram College, Thoothukudi. Professor and Head, Research Department of Physics, V. O. Chidambaram College, Thoothukudi for their extended help.

#### **FUNDING SOURCES**

This research did not receive any specific grant from funding agencies in the public, commercial, or not-for-profit sectors.

#### **CONFLICT OF INTEREST**

The authors declare that they have no known competing financial interests or personal relationships that could have appeared to influence the work reported in this paper.

#### **REFERENCES**

Afandi, G. El & Ismael, H., 2023, 'Spatiotemporal Variation of Summertime Urban Heat Island (UHI) and Its Correlation with Particulate Matter (PM<sub>2.5</sub>) over Metropolitan Cities in Alabama', *Geographies* 2023, Vol. 3, Pages 622-653, 3(4), 622-653.

- Agr Sci-Tarim Bili, J. & Aslan, V., 2024, 'Determination of Van Basin Groundwater Potential by GIS Based, AHP and Fuzzy-AHP Methods', *Journal of Agricultural Sciences*, 30(1), 47–60.
- Allan, M., Rajabifard, A. & Foliente, G., 2024, 'Climate resilient urban regeneration and SDG 11–stakeholders' view on pathways and digital infrastructures', *International Journal of Digital Earth*, 17(1).
- Aloui, S., Zghibi, A., Mazzoni, A., Elomri, A. & Al-Ansari, T., 2024, 'Identifying suitable zones for integrated aquifer recharge and flood control in arid Qatar using GIS-based multi-criteria decision-making', *Groundwater for Sustainable Development*, 25(3), 101137.
- Antony, C., Grace, Z., Soundranayagam, J.P., Antony, A., Promilton, A., Stephen Pitchaimani, V. & Roy, E.A., 2024, 'Synergizing Hazard Resilience And Renewable Energy Potential For Smart Coastal Development: A GIS-MCDA Approach In Thoothukudi, India', *Nanotechnology Perceptions*, 20(S14), 4714–4734.
- Arora, N.K. & Mishra, I., 2024, 'Life on land: progress, outcomes and future directions to achieve the targets of SDG 15', *Environmental Sustainability 2024 7:4*, 7(4), 369–375.
- Aswin, S.K., Pitchaimani, V.S. & Promilton, A.A.A., 2025, 'Flood Susceptibility Assessment for Coastal Villages of Southern Tamil Nadu: An Integrated GIS and AHP Approach', *Disaster Advances*, 18(6), 18–27.
- Bibi, T.S. & Kara, K.G., 2023, 'Evaluation of climate change, urbanization, and low-impact development practices on urban flooding', *Heliyon*, 9(1), e12955.
- Chandu, P.J., Bindu, G. & Vishnu Sharan K. J., 2025, 'Seasonal Analysis of Land Surface Temperature and Urban Heat Island Dynamics: A Comparative

- Study of Kochi and Fairbanks’, *International Journal of Environment and Climate Change*, 15(2), 544–555.
- Chaube, S., Pant, S., Kumar, Anuj, Uniyal, S., Singh, M.K., Kotecha, K. & Kumar, Akshay, 2024, ‘An Overview of Multi-Criteria Decision Analysis and the Applications of AHP and TOPSIS Methods’, *An Overview of Multi-Criteria Decision Analysis and the Applications of AHP and TOPSIS Methods*, 9(3), 581–615.
- Chowdhury, P., Lakku, N.K.G., Lincoln, S., Seelam, J.K. & Behera, M.R., 2023, ‘Climate change and coastal morphodynamics: Interactions on regional scales’, *Science of The Total Environment*, 899, 166432.
- Faheem, Z., Kazmi, J.H., Shaikh, S., Arshad, S., Noreena & Mohammed, S., 2024, ‘Random forest-based analysis of land cover/land use LCLU dynamics associated with meteorological droughts in the desert ecosystem of Pakistan’, *Ecological Indicators*, 159(4), 111670.
- Fourie, A.N., 2022, *SDG 9: Build Resilient Infrastructure, Promote Inclusive and Sustainable Industrialization and Foster Innovation*, Cambridge University Press.
- Ghosh, S. & Mistri, B., 2023, ‘Cyclone-induced coastal vulnerability, livelihood challenges and mitigation measures of Matla–Bidya inter-estuarine area, Indian Sundarban’, *Natural Hazards (Dordrecht, Netherlands)*, 116(3), 3857.
- Gomez Rave, D.V., Scolobig, A. & Jesus, M. del, 2025, ‘Review article: Rethinking Preparedness for Coastal Compound Flooding: Insights from a Systematic Review’.
- Gorelick, N., Hancher, M., Dixon, M., Ilyushchenko, S., Thau, D. & Moore, R., 2017, ‘Google Earth Engine: Planetary-scale geospatial analysis for everyone’, *Remote Sensing of Environment*, 202, 18–27.

- Halkos, G. & Argyropoulou, G., 2022, 'Using environmental indicators in performance evaluation of sustainable development health goals', *Ecological Economics*, 192, 107263.
- Huang, P., Hou, M., Sun, T., Xu, H., Ma, C. & Zhou, A., 2024, 'Sustainable groundwater management in coastal cities: Insights from groundwater potential and vulnerability using ensemble learning and knowledge-driven models', *Journal of Cleaner Production*, 442, 141152.
- Krishnan, A. & Ramasamy, J., 2024, 'Climate Change and Cyclones: Its Associated Consequences in Tamil Nadu Coastal Cities of Chennai and Thoothukudi', *Climate Change, Vulnerabilities and Adaptation: Understanding and Addressing Threats with Insights for Policy and Practice*, 47–59.
- Kumar, Rahul, Mishra, V., Buzan, J., Kumar, Rohini, Shindell, D. & Huber, M., 2017, 'Dominant control of agriculture and irrigation on urban heat island in India', *Scientific Reports* 2017 7:1, 7(1), 14054-.
- Mansour, M.M., Ibrahim, M.G., Fujii, M. & Nasr, M., 2022, 'Sustainable development goals (SDGs) associated with flash flood hazard mapping and management measures through morphometric evaluation', *Geocarto International*, 37(26), 11116–11133.
- Maqsoom, A., Aslam, B., Khalid, N., Ullah, F., Anysz, H., Almaliki, A.H., Almaliki, A.A. & Hussein, E.E., 2022, 'Delineating Groundwater Recharge Potential through Remote Sensing and Geographical Information Systems', *Water* 2022, Vol. 14, Page 1824, 14(11), 1824.
- Mitra, R., Das, J. & Kamruzzaman, M., 2023, 'Application of TOPSIS method for flood susceptibility mapping using Excel and GIS', *MethodsX*, 11, 102263.
- Nandi, S. & Swain, S., 2024, 'Role of groundwater systems in fulfilling

- sustainable development goals: A focus on SDG6 and SDG13’, *Current Opinion in Environmental Science & Health*, 42, 100576.
- Nazaripour, H., Sedaghat, M., Shafaie, V. & Movahedi Rad, M., 2024, ‘Strategic assessment of groundwater potential zones: a hybrid geospatial approach’, *Applied Water Science*, 14(8), 1–20.
- Norizan, N.Z.A., Hassan, N. & Yusoff, M.M., 2021, ‘Strengthening flood resilient development in malaysia through integration of flood risk reduction measures in local plans’, *Land Use Policy*, 102, 105178.
- Nyberg, B., Gilmullina, A., Helland-Hansen, W., Nienhuis, J. & Storms, J., 2025, ‘Global coastal exposure patterns by coastal type from 1950 to 2050’, *Cambridge Prisms: Coastal Futures*, 3, e12.
- Odiji, C., James, G., Oyewumi, A., Karau, S., Odia, B., Idris, H., Aderoju, O. & Taminu, A., 2024, ‘Decadal mapping of flood inundation and damage assessment in the confluence region of Rivers Niger and Benue using multi-sensor data and Google Earth Engine’, *Journal of Water and Climate Change*, 15(2), 348–369.
- Opricovic, S. & Tzeng, G.H., 2004, ‘Compromise solution by MCDM methods: A comparative analysis of VIKOR and TOPSIS’, *European Journal of Operational Research*, 156(2), 445–455.
- Pérez-Cutillas, P., Pérez-Navarro, A., Conesa-García, C., Zema, D.A. & Amado-Álvarez, J.P., 2023, ‘What is going on within google earth engine? A systematic review and meta-analysis’, *Remote Sensing Applications: Society and Environment*, 29, 100907.
- Purmohammadi, M.H., Eslami, H., Derikvand, E. & Babarsad, M.S., 2024, ‘Identification of Potential Groundwater Zones for Digging Underground Water Wells Using Ahp

- and Topsis Hierarchical Analysis Method in Dezful-Andimeshk Plain’.
- Qazi, A., Angell, L.C., Simsekler, M.C.E., Daghfous, A. & Al-Mhdawi, M.K.S., 2025, ‘Assessing the impact of sustainability risks on disaster and pandemic vulnerabilities: A global perspective’, *Global Transitions*, 7, 159–174.
- Richard Abishek, S. & Antony Ravindran, A., 2023, ‘Assessment of groundwater potential zones for urban development site suitability analysis in Srivaikundam region, Thoothukudi district, South India’, *Urban Climate*, 49, 101443.
- Saaty, T.L., 1987, ‘Principles of the Analytic Hierarchy Process’, *Expert Judgment and Expert Systems*, 27–73.
- Shahfahad, Talukdar, S., Naikoo, M.W., Rihan, M., Mohammad, P. & Rahman, A., 2024, ‘Seasonal dynamics of land surface temperature and urban thermal comfort with land use land cover pattern in semi-arid Indian cities: Insights for sustainable Urban Management’, *Urban Climate*, 57, 102105.
- Singha, C., Rana, V.K., Pham, Q.B., Nguyen, D.C. & Łupikasza, E., 2024, ‘Integrating machine learning and geospatial data analysis for comprehensive flood hazard assessment’, *Environmental Science and Pollution Research International*, 31(35), 48497.
- TNSDMA, T.N.S.D.M.A., 2024, *DISTRICT DISASTER MANAGEMENT PLAN 2024 for Thoothukudi District*.
- UNDP, 2025, *Disaster risk and the 2030 Agenda for Sustainable Development | UNDRR*.
- United Nations Department of Economic and Social, 2024, ‘The Sustainable Development Goals Report 2024’.
- Xu, C., Pu, L., Kong, F. & Li, B., 2021, ‘Spatio-Temporal Change of Land Use in a Coastal Reclamation Area: A Complex Network Approach’,

*Sustainability* 2021, Vol. 13, Page  
8690, 13(16), 8690.

Xue, C., Yang, G., Ma, X., Zhen, J., Sun,  
H., Zhang, X., Ruan, X., Jiang, H. &  
Shou, W., 2024, 'Mapping Compound  
Flooding Risks for Urban Resilience  
in Coastal Zones: A Comprehensive  
Methodological Review', *Remote  
Sensing* 2024, Vol. 16, Page 350,  
16(2), 350.

Zhu, Q. & Abdelkareem, M., 2021,  
'Mapping Groundwater Potential  
Zones Using a Knowledge-Driven  
Approach and GIS Analysis', *Water*  
2021, Vol. 13, Page 579, 13(5), 579.

Zope, P.E., Eldho, T.I. & Jothiprakash, V.,  
2015, 'Impacts of urbanization on  
flooding of a coastal urban catchment:  
a case study of Mumbai City, India',  
*Natural Hazards*, 75(1), 887–908.